Denis Goldnik
Philipp Lösch*
Siegfried Ripperger
Kai Nikolaus
Sergiy Antonyuk

Diafiltration of Highly Concentrated Suspensions with Fine Particles by Dynamic Disk Filtration

A method for washing highly concentrated suspensions with fine particles by using a filter with overlapping disks was studied. For the experiments, alumina and titanium dioxide suspensions were used. It was demonstrated that the used suspensions have non-Newtonian behavior. The viscosity is influenced by the type of particle system, the solid concentration, and the shear rate. The washing process is operated in a discontinuous and a continuous way. The rotation of the disks and the shear flow across their surface prevents the formation of a filter cake and facilitates the handling of suspensions. The shear stresses at the filter disk and the rheology of the processed suspensions are both influenced by the type of particle system, the solid concentration, and the process parameters.

Keywords: Disk filters, Disk separators, Dynamic washing, Viscosity of suspensions, Washing of suspensions

Received: May 07, 2021; *revised:* June 04, 2021; *accepted:* August 25, 2021

DOI: 10.1002/ceat.202100194

1 Introduction

Washing of suspensions or filter cakes includes the removal of the mother liquor surrounding the particles with a suitable washing fluid. The mother liquor often contains solute substances. These can be undesirable pollutants in the final product or a valuable byproduct which should be separated. The washing occurs mostly in combination with concentration of the suspension.

In the pharmaceutical industry, often minimal residual concentrations of the mother liquor in the concentrated suspension are demanded. Therefore, the choice of the correct washing procedure is of great importance. At this point, the properties of the particle system and the mother liquor must always be considered. Hoffner et al. give an overview of the washing procedures and their optimal fields of application [1].

The washing of colloidal particle systems often causes multiple difficulties. Erk [2] and Alles [3] showed that colloidal systems often form a compressible filter cake with high flow resistance, entailing long filtration and washing times. Furthermore Wiedemann and Stahl reported on the high risk of cracking in compressible filter cakes, which leads to inhomogeneous flow and high consumption of washing liquid [4]. If porous particle systems are used, the difficulties increase, as mother liquor can remain in the inner pores of the particles [5].

Heuser [6], who examined the jet washing of thin cakes with low porosity, redispersed the filter cake during washing. Hieke et al. [7] performed the filtration of colloidal particle systems with thin filter cakes. Hoffner and Stahl [8] developed an apparatus with one or several washing chambers connected in series. The highly concentrated suspension moves through the chambers like a bulk material.

Alternatively to these procedures, the washing process can be performed directly with a concentrated suspension. This method is called diafiltration [9]. Diafiltration can be implemented in a continuous or discontinuous way. During a discontinuous diafiltration, the suspension is concentrated to a certain degree. Afterwards, the volume of the removed mother liquor is replaced by the washing liquid, and concentration of the suspension is started again. This process is repeated periodically. For the continuous implementation, the volume of the removed mother liquor is replaced continuously by the washing fluid, so that the particle concentration of the suspension is constant during the process.

In this work, the discontinuous and continuous diafiltration of highly concentrated dispersed suspensions was studied with dynamic filters with overlapping rotating disks. The disks are arranged on hollow shafts [10–13] and form a gap between the disks. In the gap, the wall shear stress is very high and dynamic diafiltration with highly concentrated suspensions is realizable.

The rheology of suspensions with fine particles, which often exhibit non-Newtonian behavior [14], significantly influences the efficiency of the diafiltration process and the energy demand. Therefore, the rheological properties of alumina and titanium dioxide suspensions used in the diafiltration study were obtained experimentally.

Denis Goldnik, Philipp Lösch, Prof. Dr.-Ing. Siegfried Ripperger, Dr.-Ing. Kai Nikolaus, Prof. Dr.-Ing. Sergiy Antonyuk
philipp.loesch@mv.uni-kl.de
Technische Universität Kaiserslautern, Institute of Particle Process Engineering, Gottlieb-Daimler-Strasse 44, 67663 Kaiserslautern, Germany.

2 Theoretical Description of Filters with Rotating Disks

Filters with rotating overlapping disks are arranged on two or more hollow shafts and mutually overlap (Fig. 1). The disks have open ducts on the inside for the radial filtrate discharge, so that the filtrate can leave via the hollow shafts. The rotation direction of the shafts is chosen such that the disks in the shear gap move opposite to each other. Thereby, the suspension in the gap is sheared and the buildup of a filter cake is hindered. In the case of the same rotational speed of each disk, the relative speed in the shear gap is constant. Ceramic disks are available with a diameter up to 300 mm. The pore sizes are in the range of microfiltration and ultrafiltration. Other disks are made of stainless steel or can be coated with a polymer membrane.

Many authors theoretically described the forces which act on particles near the surface during suspension flow [15–24]. In other works the forces were examined experimentally [25–29]. The permeate drag acts parallel to the movement direction of the filtrate (Eq. (1)) [30].

$$F_D = F_{Stokes}\lambda_S(x_p,\phi) = 3\pi\eta_f x_p v_f \lambda_S(x_p,\phi) \quad (1)$$

where η_f[1)] is the dynamic fluid viscosity, x_p the diameter of the followed particle, v_f the velocity of the permeate flux, and λ_s the hydrodynamic correction factor to the Stokes drag force F_{Stokes}, which is dependent on the particle diameter x_p and particle volume concentration ϕ.

The permeate drag causes accumulation of the particles close to the disk surface. The accumulation is counteracted by the lift force on the particles, which can be expressed according to Saffman [22] as (Eq. (2)):

$$F_L = 0.761\frac{\tau_w^{1.5}x_p^3\rho_p^{0.5}}{\eta_f} \quad (2)$$

The lift force is caused by the shear flow and is influenced by the wall shear stress τ_w, x_p, the particle density ρ_p and the dynamic fluid viscosity η_f.

Therefore, a dynamic equilibrium of deposition and detachment of particles occurs close to the surface. This equilibrium is determined by the wall shear stress τ_w and the transmembrane pressure [31]. The size-dependent particle deposition and its description using the equilibrium of hydrodynamic forces were experimentally investigated in cross-flow filtration in previous works [32, 33]. In contrast to the classical cross-flow filtration, the wall shear stress does not exclusively depend on the cross-flow velocity of the suspension. The wall shear stress is primarily influenced by the rotational speed n of the disks. Therefore, relatively high wall shear stresses can be realized at low pressure differences.

This condition is desirable for particle systems which can form compressible layers, as the flow rate exhibits a maximum at a certain pressure difference [34]. The pressure and flow

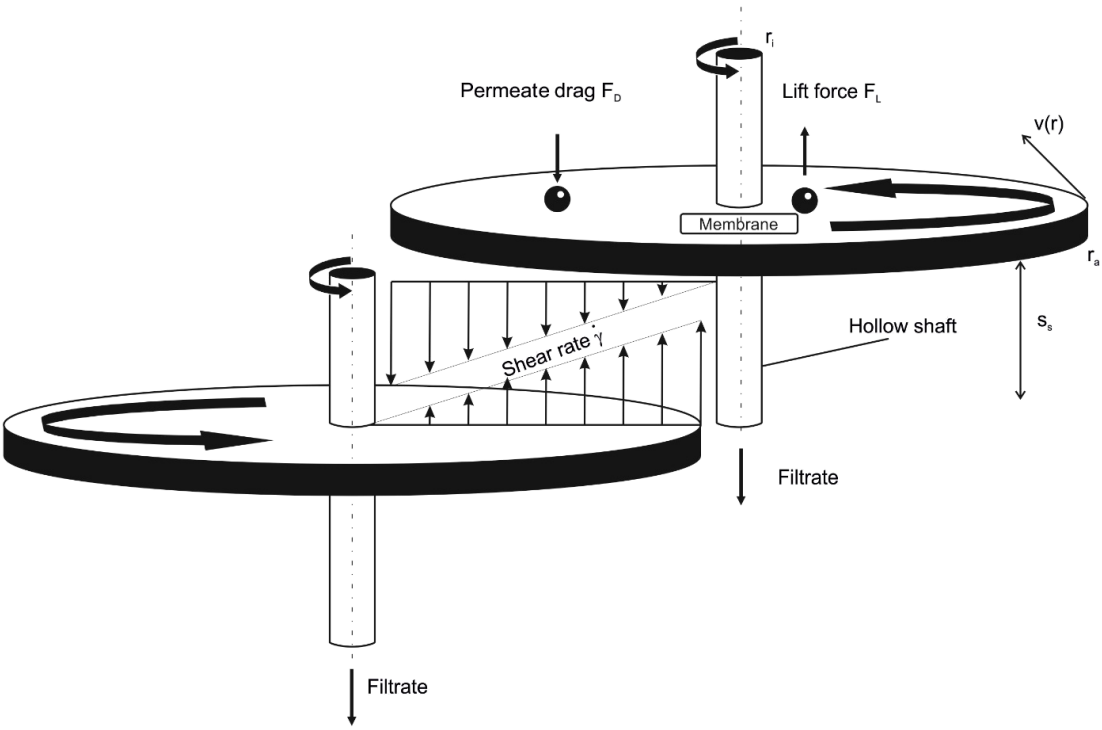

Figure 1. Forces and flow conditions in the gap between two overlapping disks.

1) List of symbols at the end of the paper.

conditions vary along the disk radius *r*. Kracht [35], Tonhäuser et al. [36], Daily and Nece [37], Cooper and Reshotko [38], Ketola and McGrew [39], and Schiele [40] stated that the fluid flow on rotating disks can have laminar and turbulent areas due to the tangential velocity. The shear rate of filters with one disk is dependent on the radius. Disk filters with overlapping disks compensate the irregular fluid flow areas. In these filters, the overlapping disks have the same direction of rotation. This causes a shear of the suspension between the disks (Fig. 1). Due to the same rotational speed of both disks, the shear rate $\dot{\gamma}$ in the gap between disks (distance s_s) is independent of the radius and can be calculated by using the inner and outer radii r_a and r_i (Eq. (3)):

$$\dot{\gamma} = \frac{v(r_a) + v(r_i)}{s_s} \tag{3}$$

For the description of the washed-out salt concentration in the suspension, the dimensionless concentration c^* can be used (Eq. (4)):

$$c^* = \frac{c_s}{c_0} \tag{4}$$

where c_s is the actual and c_0 the initial concentration of the salt. The washing process can be operated in a discontinuous and a continuous way. In discontinuous diafiltration, the initial suspension with volume V_0 is concentrated to a certain volume V_{sus}, and then, the mother liquor discharged through filtration is replaced by the washing liquid. This procedure is repeated *m* times. The concentration gradient of the removed substance can be modeled by Eq. (5):

$$c^* = \left(\frac{V_{sus}}{V_0}\right)^m \tag{5}$$

During continuous diafiltration, the concentration of particles in the suspension does not change. The discharged mother liquor is continuously replaced by the washing liquid. Therefore, a constant stream of washing liquid can be achieved. Continuous diafiltration can be described by Eq. (6):

$$c^* = e^{-\left(\frac{V_w}{V_{sus}}\right)} \tag{6}$$

where V_w is the added volume of washing fluid.

The washing process with rotating disk filter can be modeled as a continuous diafiltration. Diafiltration in rotating disks at small suspension volume can be modeled as a stirred tank reactor. In this case, the volume of the washing fluid can be calculated from Eq. (7) independently of the operation mode.

$$V_w = -\ln(c^*)V_{sus} \tag{7}$$

3 Experimental Investigations

3.1 Preparation of the Suspension

For the diafiltration experiments, suspensions of alumina (Al_2O_3, Almatis GmbH, CT 3000) and titanium dioxide (TiO_2, Venator Germany GmbH, R 611) were used. To investigate the washing progress, sodium chloride was used as model pollutant. The suspension consisting of the continuous phase of water and sodium chloride in molar ratio of 0.1 and the solid phase of Al_2O_3 or TiO_2 was prepared by using an Ultra Turrax homogenizer and ultrasonication for 10 min.

The particle size distributions of the dispersed solids were measured with a Horiba LA 950 laser diffraction spectrometer (Retsch GmbH). The observed suspensions both had a pH of 8.5. Fig. 2 shows the particle size distribution of the prepared Al_2O_3 and TiO_2 suspensions. The particle size distribution of Al_2O_3 ranged from 0.1 to 10 µm with mass-related modal value $x_{50,3}$ of 3.5 µm. The used TiO_2 suspension contained substantially finer particles in the range of 0.1 to 2.0 µm with an modal $x_{50,3}$ value of 0.4 µm.

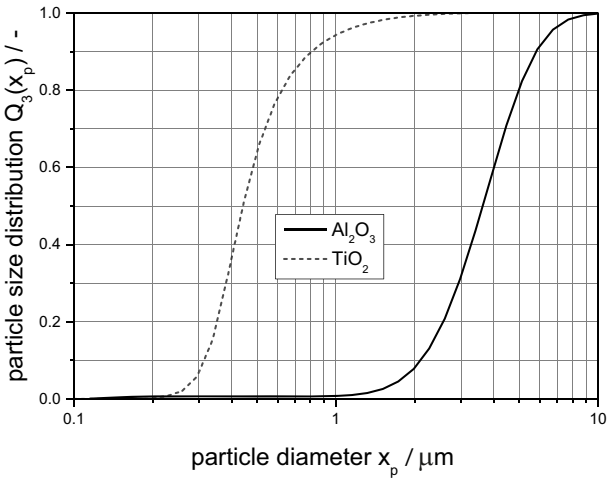

Figure 2. Cumulative particle size distributions Q_3 of the Al_2O_3 and TiO_2 suspensions.

The rheology of the suspensions significantly influenced the efficiency of the washing process. The rheological behavior of the suspensions was characterized by using a HAAKE RheoStress 6000 rotational rheometer with a parallel plate shearing geometry, which is preferred for high-viscosity liquids. The viscosity measurements on suspensions were performed by varying solid volume concentrations between $\phi = 0.1$ and $\phi = 0.37$. The measurements were performed with ascending and descending shear rates. The shear rate was varied between $\dot{\gamma} = 10\,s^{-1}$ and $\dot{\gamma} = 500\,s^{-1}$. The suspension temperature was constant at $\vartheta = 20\,°C$. Each measurement was repeated once. Figs. 3 and 4 show the viscosity of Al_2O_3 and TiO_2 suspensions, respectively, in dependence on the shear rate $\dot{\gamma}$ and volume concentration ϕ.

The measurements indicate that highly concentrated Al_2O_3 and TiO_2 suspensions have a non-Newtonian, pseudoplastic behavior. The suspension viscosities increase with increasing volume concentration of the solid phase and decrease with increasing shear rate. Regarding the short measurement intervals of each shear rate, an expectable thixotropic behavior could not be observed and is therefore not relevant in regard to the short washing intervals.

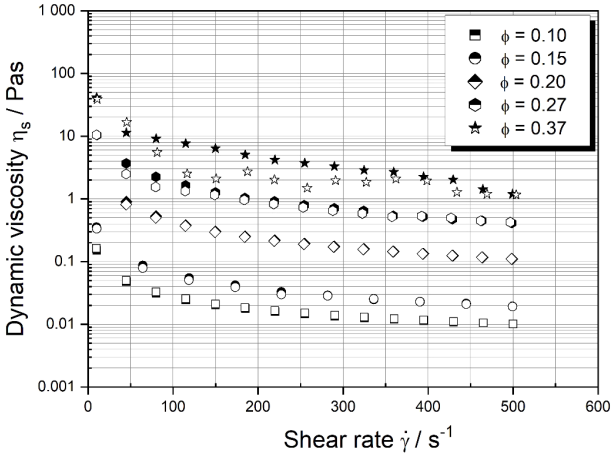

Figure 3. Viscosity of Al_2O_3 suspensions with ϑ = 20 °C depending on the shear rate $\dot{\gamma}$ and the volume concentration ϕ. Full symbols: values measured with ascending shear rate. Empty symbols: values measured with descending shear rate.

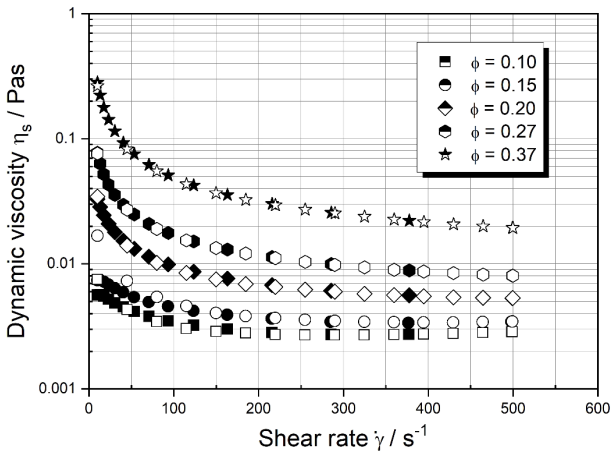

Figure 4. Viscosity of TiO_2 suspensions with ϑ = 20 °C depending on the shear rate $\dot{\gamma}$ and the volume concentration ϕ. Full symbols: values measured with ascending shear rate. Empty symbols: values measured with descending shear rate.

The measured suspension viscosities can be approximated by the model of Herschel and Bulkley [41].

$$\tau = \tau_0 + K\dot{\gamma}^{n^*} \tag{8}$$

where τ_0 is the initial yield stress, K the consistency index, $\dot{\gamma}$ the shear rate, and n^* the flow coefficient.

Fig. 5 shows the shear stress in dependence on the shear rate $\dot{\gamma}$ and volume concentration ϕ for Al_2O_3 suspensions. The Al_2O_3 suspensions exhibit an initial yield stress τ_0, which increases with increasing volume concentration of the solid phase.

Tab. 1 shows the obtained parameters of the Herschel-Bulkley model for the measured Al_2O_3 suspensions. A higher volume concentration causes an increase of the initial yield stress and the apparent dynamic viscosity. The flow coefficient

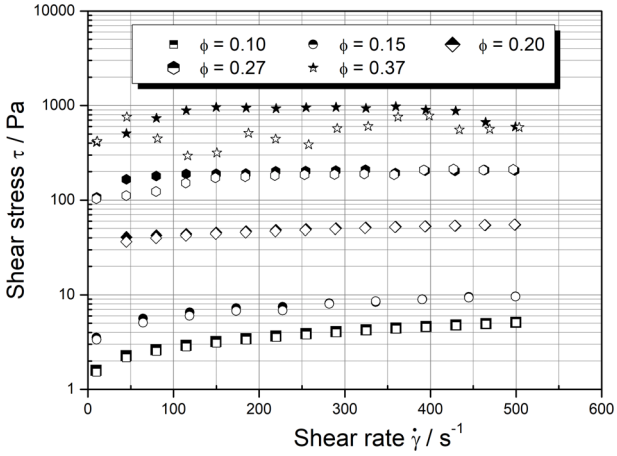

Figure 5. Shear stress depending on the shear rate $\dot{\gamma}$ and the volume concentration ϕ for Al_2O_3 suspensions with ϑ = 20 °C.

Table 1. Rheological parameters of Al_2O_3 suspensions.

ϕ [%]	τ_0 [Pa]	K [Pa s^n]	n^* [–]
10	1.2	0.12	0.57
15	2.0	0.55	0.42
20	29.0	2.35	0.39
27	41.8	3.08	0.37
37	429.5	46.41	0.31

decreases with increasing volume concentration of the particles.

In filtration processes, low viscosities are desirable. Therefore diafiltration experiments were conducted at a high shear rate of $\dot{\gamma}$ = 3543 s^{-1}. The rotation of the overlapping filter disks caused high wall shear stress, which led to a low viscosity of the non-Newtonian pseudoplastic suspensions. The high wall shear stress led to high lift forces on the particles, which reduced the deposition of particles on the filter surface. Furthermore the centrifugal force reduced the formation of high deposition layers.

3.2 Experimental Setup

The continuous and discontinuous diafiltration of Al_2O_3 and TiO_2 suspensions was conducted with a dynamic Krauss-Maffei cross-flow filter DCF 152/0,14 from Andritz KMPT. This filter consists of two horizontal hollow shafts on which six disks are installed. Fig. 6 shows the arrangement of the filter disks in the filter. The axial gap between the overlapping filter disks is 4 mm. To prevent the influence of uneven shear stress on the outer disks, the two outer disks are made from steel and thus impermeable and only ensure regular shear stress on the outside of the inner disks. The four inner disks are ceramic membranes with an average pore diameter of 0.2 µm. The outer diameter of

Figure 6. Arrangement of the filter disks in the DCF 152/0,14 filter [42].

a disk is 152 mm, and the inner diameter is 40 mm. The total filter surface of the four permeable disks is $A_f = 0.14\ m^2$. The maximum disk rotation speed is $n = 1410\ min^{-1}$.

Fig. 7 shows a detailed layout of the experimental setup. The prepared suspension was added in a tempered and agitated storage tank. The suspension was delivered from the storage tank into the disk filter by a pump. The concentrated suspension exited the filter and returned to the storage tank. For the process control, several sensors were installed:

- flow meters for the concentrated suspension (retentate) and the filtrate (ABB miniflow),
- pressure sensors for the suspension (feed) and the filtrate (PF2054, ifm electronic),
- a temperature sensor for the filtrate (ProMinent Dulcotest PT100).

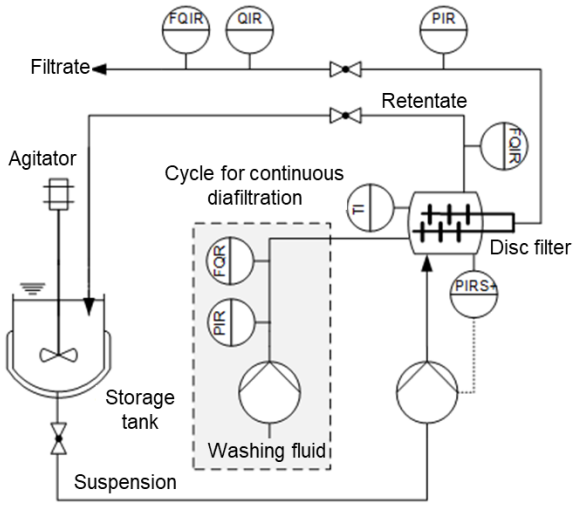

Figure 7. The experimental setup with measurement and control sensors.

A conductivity measurement cell (ProMinent Dulcometer DMTa with LMP 1) in the filtrate channel provided information about the sodium chloride concentration and showed the washing progress. The pressure difference between the filter housing and filtrate channel was for all experiments $\Delta p = 1$ bar.

4 Experimental Results

For the investigations of diafiltration, Al_2O_3 and TiO_2 suspensions were washed periodically at a constant temperature of $\vartheta = 20\,°C$ and rotational speed of $n = 1400\ min^{-1}$. From the initial suspension volume of $V_0 = 10.5$ L a filtrate volume of 2 L was removed, which led to an increase of the particle concentration in the the suspension from $\phi_0 = 0.14$ to $\phi_{sus} = 0.17$. Afterwards, the filtrate volume was substituted by the washing fluid. This procedure was repeated m times, depending on the washing fluid volume, to reach a salinity of $c^* = 0.01$.

Fig. 8 shows the filtrate flow rate during the washing time for Al_2O_3 and TiO_2. The filtrate flows increased during the first 200 s of the experiments and remained nearly constant during the washing time t_w. During the first seconds the deposition layer was formed. Afterwards, the filtrate flow rate fluctuated slightly during the washing time. The mean filtrate flow remained relatively constant, which indicated that the deposition layer and its flow resistance also remained constant. The fluctuation is noticeable in the pressure curve as well. This fact was also observed by Steinke and Ripperger [43]. One possible reason contributing to the variation is the fact that the disks have a slight inclination with respect to the hollow shaft on which they are mounted. Therefore, a periodic backwash of the filter media is possible. Steinke and Ripperger introduced this procedure under the designation "autodynamic high-frequency backwashing". The average filtrate flow rate of the Al_2O_3 suspension was ca $320\ L\,h^{-1}m^{-2}$. With $113\ L\,h^{-1}m^{-2}$, the average filtrate flow of the TiO_2 suspension was significantly lower. The difference in filtrate flows of Al_2O_3 and TiO_2 can be explained by the different particle size distributions of the particle systems. It can be assumed that the finer TiO_2 particles form a denser deposition layer. The smaller particle size and porosity of the particles in the layer resulted in higher flow resistance.

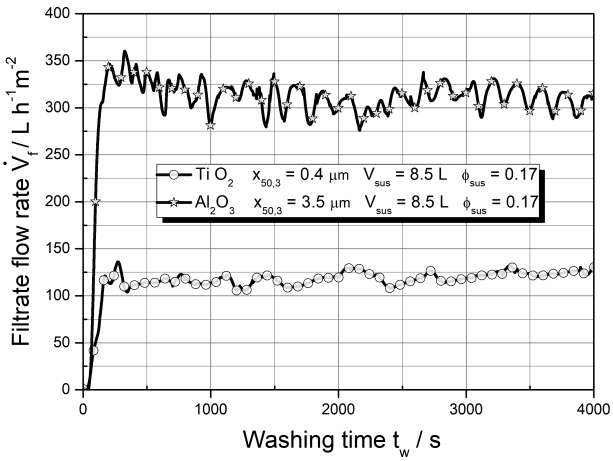

Figure 8. Filtrate flow rate for TiO_2 and Al_2O_3 suspensions with $V_0 = 10.5$ L, $\phi_0 = 0.14$, $\vartheta = 20\,°C$, and $n = 1400\ min^{-1}$.

For comparison of the continuous and discontinuous washing processes, the volume of the washing fluid and the washing time were obtained. In the performed experiments, Al_2O_3 suspensions with an initial volume of V_0 = 14 L and a concentration of ϕ_0 = 0.2 were filtered to generate a constant deposition layer. The temperature of the suspension and the rotation speed were ϑ = 20 °C and n = 1400 min^{-1}, respectively. For both operation modes, the suspensions were reduced to a volume of V_{sus} = 12 L or V_{sus} = 8 L before the washing fluid was added. This caused an increase of the initial volume concentration of ϕ_0 = 0.2 to ϕ_{sus} = 0.23 and ϕ_{sus} = 0.33, respectively. Afterwards, the continuous or discontinuous washing process was started. The measured data were approximated by Eqs. (5) and (6). Fig. 9 shows the measured and approximated washing fluid volume depending on the dimensionless residual concentration for continuous and discontinuous diafiltration.

The comparison shows that the initial concentration has an influence on the volume of the washing fluid. For both operation modes, the concentrated Al_2O_3 suspension with V_{sus} = 12 L and ϕ_{sus} = 0.23 needed a washing fluid volume of $V_w \approx$ 55 L to reach a residual salinity of c^* = 0.01. In the case of a higher concentration of ϕ_{sus} = 0.33, a washing fluid volume of V_w = 37 L was obtained. With a higher initial concentration, it was possible to save 33 % of the washing fluid.

A different initial concentration causes a different filtrate flow because of the different resistance of the built deposition layer. The filtrate flow rate determines the kinetics of the washing process. With increasing filtrate flow, the replacement of the mother liquor by the washing fluid occurs faster. This is shown in Fig. 10 for the discontinuous and continuous washing process of Al_2O_3 suspensions at ϑ = 20 °C, n = 1400 min^{-1}, ϕ_0 = 0.2, and V_0 = 14 L. For the discontinuous and continuous washing, the first concentration step from ϕ_0 = 0.2 to ϕ_{sus} = 0.23 and ϕ_0 = 0.33, respectively, caused a decrease of the filtrate flow rate. After the concentration increase and the layer buildup, the continuous or discontinuous addition of the washing fluid took place. In case of a discontinuous operation an increase of the initial concentration from ϕ_0 = 0.2 to ϕ_{sus} = 0.23 during the washing steps caused a small decrease of the average filtrate flow rate from $\dot{V}_f \approx$ 210 Lh^{-1}m^{-2} to $\dot{V}_f$ = 200 Lh^{-1}m^{-2}. The duraton of the washing steps was 300 s.

The discontinuous diafiltration of the initial concentration from ϕ_0 = 0.2 to ϕ_{sus} = 0.33 significantly reduced the filtrate flow rate from $\dot{V}_f \approx$ 170 Lh^{-1}m^{-2} to $\dot{V}_f$ = 50 Lh^{-1}m^{-2}. After adding washing fluid the filtrate flow rate increased again to $\dot{V}_f$ = 170 Lh^{-1}m^{-2}. This occurred periodically every 1000 s.

For the discontinuous diafiltration, the filtrate flow decreased during the concentrating step. While continuously adding washing fluid, the filtrate flow increased steadily. Thus, the continuous diafiltration required less washing time. A reason for this increase is a higher wall shear stress, which is affected by the amount of the continuous volume stream of the washing fluid. These factors reduced the thickness of the deposit layer.

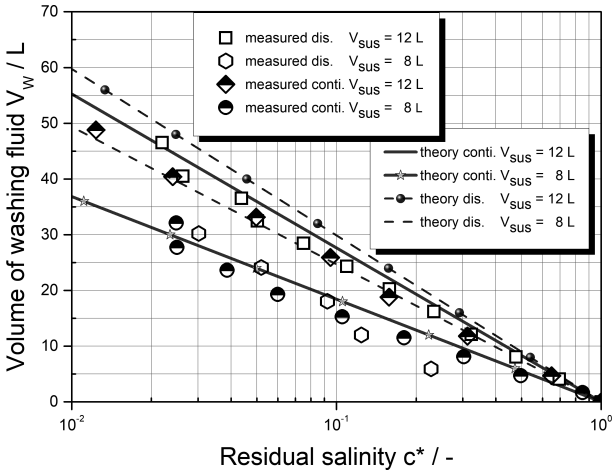

Figure 9. Volume of washing fluid for continuous and discontinuous washing for an Al_2O_3 suspension with V_0 = 14, ϕ_0 = 0.2, ϑ = 20 °C, and n = 1400 min^{-1}.

The washing fluid volume can be calculated from the average filtrate flow rate $\dot{V}_f$, the surface area A_f, and the washing time t_w as Eq (9):

$$V_w = \overline{\dot{V}_f} A_f t_w \tag{9}$$

The average filtrate flow rate was determined experimentally from the approximately constant volume flow rate. With Eqs. (7)–(9) the washing time can be calculated as a function of the residual salinity (Eq. (10)):

$$t_w = -\frac{\ln(c^*) V_{sus}}{\overline{\dot{V}_f} A_f} \tag{10}$$

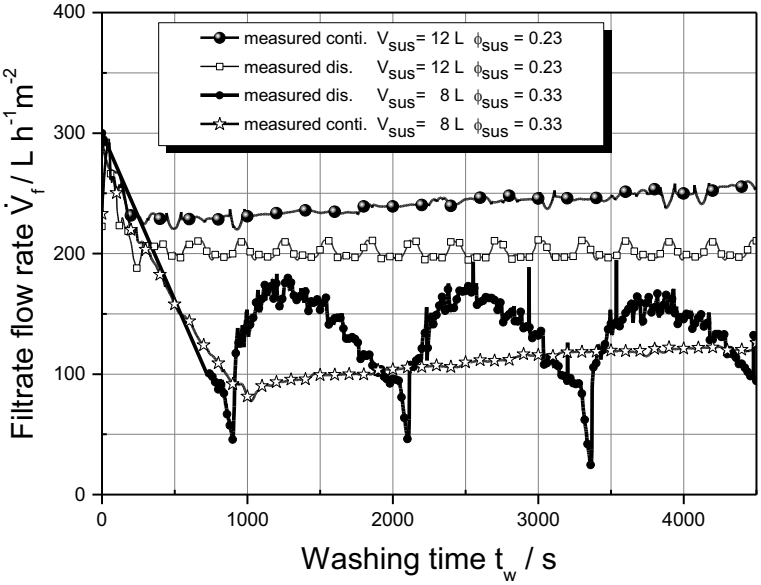

Figure 10. Filtrate flow rate in dependence on the operation mode for concentrated Al_2O_3 suspensions with ϕ_{sus} = 0.23 and ϕ_{sus} = 0.33.

The calculated and measured washing times are compared in Fig. 11 for the discontinuous washing processes of Al_2O_3 suspensions at ϑ = 20°C, n = 1400 min^{-1}, ϕ_0 = 0.2, and V_0 = 14 L. The average filtrate flow rate for the discontinuous diafiltration in which the volume was reduced to V_{sus} = 12 L was $\dot{V}_f$ = 205 L h^{-1}m^{-2} (see Fig. 10). The diafiltration with a reduced volume of V_{sus} = 8 L had an average filtrate flow rate of $\dot{V}_f$ = 110 L h^{-1}m^{-2}. Fig. 11 shows a good agreement between the calculated and experimental results. During the washing process the high concentrated Al_2O_3 suspension with V_{sus} = 12 L reaches a residual salinity of c^* = 0.01 at $t_w \approx$ 7000 s, which is 30 % faster than the Al_2O_3 suspension with V_{sus} = 8 L.

A higher concentration of the Al_2O_3 suspension saved up to 33 % of the washing fluid. This caused an increase of the washing time of up to 30 %.

5 Conclusion

The washing process with a rotating disk filter was investigated for highly concentrated suspensions. The rheology of the used suspensions and its dependence on the particle concentration significantly influenced the efficiency of the washing process. The rheological characterization of the Al_2O_3 and TiO_2 suspensions performed with a rotational rheometer showed that they had a pseudoplastic behavior at volume concentrations of solids between 0.1 and 0.37. This flow behavior was described by the model of Herschel and Bulkley. The suspension viscosity increases with increasing volume concentration of the solid phase. Since in the filtration process a low viscosity is desirable, high shear rates facilitate the handling of highly concentrated suspensions. The rotation of the disks and thus the shear flow across their surface prevent the formation of high deposition layers. The average filtrate flow rate of the Al_2O_3 suspension was approximately 320 L h^{-1}m^{-2}. This was three times higher than the average filtrate flow rate of the TiO_2 suspension. This difference can be explained by the different particle size distributions of the particle systems. TiO_2 is finer and forms a deposit layer with a higher flow resistance.

The washing process with the rotating disk filter was studied for discontinuous and continuous operation. Both processes can be modeled as continuous diafiltration. A higher particle concentration of the suspension caused a lower filtrate flow rate for continuous or discontinuous operation. The model reveals that a more highly concentrated suspension with a smaller fraction of the mother liquid reduces the volume of washing fluid needed to reach a defined residual salinity. The more highly concentrated suspensions saved 33 % of the washing fluid for a residual salinity of c^* = 0.01. This increased the washing time by up to 30 %.

The washing time to reach a residual concentration was calculated. Continuous diafiltration requires a shorter washing time than discontinuous diafiltration. The reason for the shorter washing time is the higher wall shear stress, which is due to the continuous volume stream of the washing fluid and therefore a constant viscosity of the suspension.

Acknowledgment

The studies for the rheological behaviour of suspensions were funded by the Deutsche Forschungsgemeinschaft (DFG, German Research Foundation) and the French Agence Nationale de la Recherche (ANR) and DFG collaboration project "PASTFLOW" (DFG project-ID 431419392, ANR-19-CE08-0030), which the authors gratefully acknowledge. Open access funding enabled and organized by Projekt DEAL.

The authors have declared no conflict of interest.

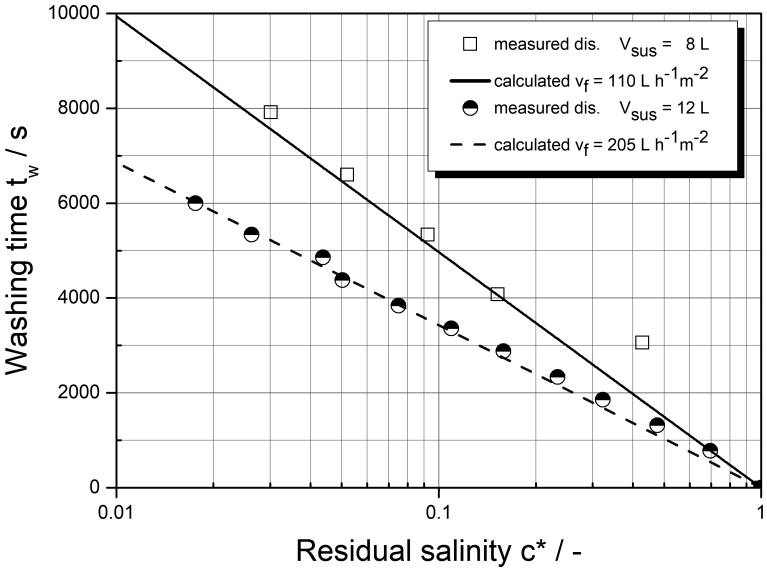

Figure 11. Filtrate flow rate in dependence on the operation mode for concentrated Al_2O_3 suspensions with ϕ_{sus} = 0.23 and ϕ_{sus} = 0.33.

Symbols used

A_f	[m^2]	filter surface area
c^*	[–]	residual salinity
c_s	[mol L^{-1}]	concentration of the substance washed out
c_0	[mol L^{-1}]	initial concentration of the substance washed out
F_D	[N]	permeate drag force
F_L	[N]	lift force
F_{Stokes}	[N]	Stokes drag force
K	[Pa s^n]	consistency index
m	[–]	number of washing steps
n	[min^{-1}]	rotation speed
n^*	[–]	rheological exponent
Δp	[bar]	transmembrane pressure
Q_3	[–]	cumulative particle size distribution
r	[mm]	radius
r_a	[mm]	outer radius
r_i	[mm]	inner radius
s_s	[mm]	axial gap between two disks
t_w	[s]	washing time

v_f	[m s^{-1}]	velocity of the filtrate flow
$\underline{\dot{V}}_f$	[L h^{-1}m^{-2}]	filtrate flow rate
$\dot{V}_f$	[L h^{-1}m^{-2}]	average filtrate flow rate
V_{sus}	[L]	volume of the concentrated suspension
V_w	[L]	volume of the washing fluid
V_0	[L]	initial volume of the suspension
x_p	[µm]	particle diameter
$x_{50,3}$	[µm]	median of the particle size distribution

Greek letters

$\dot{\gamma}$	[s^{-1}]	shear rate
η	[Pa s]	dynamic viscosity
η_{sus}	[Pa s]	dynamic viscosity of the fluid
ϑ	[°C]	temperature of the suspension
λ_s	[–]	hydrodynamic correction factor to the Stokes drag force
ρ_p	[kg m^{-3}]	particle density
τ_w	[N]	wall shear stress
τ_0	[N]	yield point
ϕ	[–]	volume concentration
ϕ_{sus}	[–]	volume concentration of the concentrated suspension
ϕ_0	[–]	initial volume concentration

References

[1] B. Hoffner, B. Fuchs, J. Heuser, *Chem. Eng. Technol.* **2004**, *27 (10)*, 1065–1071. DOI: https://doi.org/10.1002/ceat.200406142

[2] A. Erk, *Dissertation*, Universität Karlsruhe (TH) **2006**.

[3] C. M. Alles, *Dissertation*, Universität Karlsruhe (TH) **2000**.

[4] T. Wiedemann, W. Stahl, *Chem. Eng. Process.* **1996**, *35 (1)*, 35–42. DOI: https://doi.org/10.1016/0255-2701(95)04105-2

[5] S. Seupel, U. A. Peuker, *Chem. Ing. Tech.* **2019**, *91 (12)*, 1842–1852. DOI: https://doi.org/10.1002/cite.201900074

[6] J. Heuser, *Filterkuchenwaschprozesse unter besonderer Berücksichtigung physikalisch-chemischer Einflüsse, Dissertation*, Universität Karlsruhe (TH) **2003**.

[7] M. Hieke, J. Ruland, H. Anlauf, H. Nirschl, *Chem. Eng. Technol.* **2009**, *32 (7)*, 1095–1101. DOI: https://doi.org/10.1002/ceat.200800609

[8] B. Hoffner, W. Stahl, *Fluid/Part. Sep. J.* **2003**, *15 (2)*, 113–120.

[9] W. F. Blatt, S. M. Robinson, *Anal. Biochem.* **1968**, *26 (1)*, 151–173.

[10] M. Y. Jaffrin, *Curr. Opin. Chem. Eng.* **2012**, *1 (2)*, 171–177. DOI: https://doi.org/10.1016/j.coche.2012.01.002

[11] T. A. Malinovskaya, O. S. Kirsanov, V. V. Reinfart, M. Schtscherbakowa, *Chem. Tech.* **1971**, *23 (9)*, 528–531.

[12] T. A. Malinovskaya, J. A. Kobrinskij, V. Shevchenko, *Chem. Tech.* **1972**, *24 (12)*, 748–750.

[13] M. Y. Jaffrin, *J. Membr. Sci.* **2008**, *324 (1–2)*, 7–25. DOI: https://doi.org/10.1016/j.memsci.2008.06.050

[14] T. Mladenchev, *Dissertation*, Universität Magdeburg **2007**.

[15] R. G. Cox, H. Brenner, *Chem. Eng. Sci.* **1968**, *23 (2)*, 147–173. DOI: https://doi.org/10.1016/0009-2509(68)87059-9

[16] K. Bauckhage, *Chem. Ing. Tech.* **1983**, *55 (9)*, 734–735. DOI: https://doi.org/10.1002/cite.330550921

[17] C. K. W. Tam, *J. Fluid Mech.* **1969**, *38 (3)*, 537–546. DOI: https://doi.org/10.1017/S0022112069000322

[18] A. J. Goldman, R. G. Cox, H. Brenner, *Chem. Eng. Sci.* **1967**, *22 (4)*, 637–651. DOI: https://doi.org/10.1016/0009-2509(67)80047-2

[19] M. E. O'Neill, *Chem. Eng. Sci.* **1968**, *23 (11)*, 1293–1298. DOI: https://doi.org/10.1016/0009-2509(68)89039-6

[20] D. A. Drew, R. T. Lahey, *Int. J. Multiphase Flow* **1990**, *16 (6)*, 1127–1130. DOI: https://doi.org/10.1016/0301-9322(90)90110-5

[21] D. A. Drew, J. A. Schonberg, G. Belfort, *Chem. Eng. Sci.* **1991**, *46 (12)*, 3219–3224. DOI: https://doi.org/10.1016/0009-2509(91)85023-Q

[22] P. G. Saffman, *J. Fluid Mech.* **1965**, *22 (2)*, 385–400.

[23] J. B. McLaughlin, *J. Fluid Mech.* **1993**, *246*, 249–265. DOI: https://doi.org/10.1017/S0022112093000114

[24] H. Nirschl, S. Polzer, *Chem. Ing. Tech.* **1996**, *68 (4)*, 409–412. DOI: https://doi.org/10.1002/cite.330680408

[25] D. Hall, *J. Fluid Mech.* **1988**, *187*, 451–466. DOI: https://doi.org/10.1017/S0022112088000515

[26] D. A. Drew, R. T. Lahey Jr., *Int. J. Multiphase Flow* **1987**, *13 (1)*, 113–121. DOI: https://doi.org/10.1016/0301-9322(87)90011-5

[27] G. Rubin, *Dissertation*, Universität Karlsruhe (TH) **1977**.

[28] J. A. Levesley, B. J. Bellhouse, *Chem. Eng. Sci.* **1993**, *48 (21)*, 3657–3669. DOI: https://doi.org/10.1016/0009-2509(93)81022-N

[29] J. Altmann, *Dissertation*, Technische Universität Dresden **2000**.

[30] H. C. Brinkman, *Appl. Sci. Res.* **1949**, *1 (1)*, 1045. DOI: https://doi.org/10.1007/BF02120313

[31] J. Altmann, S. Ripperger, *Chem. Ing. Tech.* **1996**, *68 (10)*, 1303–1306. DOI: https://doi.org/10.1002/cite.330681013

[32] P. Lösch, K. Nikolaus, S. Antonyuk, *Chem. Ing. Tech.* **2019**, *91 (11)*, 1656–1662. DOI: https://doi.org/10.1002/cite.201900052

[33] P. Lösch, S. Antonyuk, *Powder Technol.* **2021**, *388*, 305–317. DOI: https://doi.org/10.1016/j.powtec.2021.04.043

[34] R. Berndt, J. Krippenstapel, *Chem. Ing. Tech.* **1997**, *69 (4)*, 472–475. DOI: https://doi.org/10.1002/cite.330690408

[35] D. Kracht, *Dissertation*, Martin-Luther-Universität Halle-Wittenberg **1996**.

[36] M. Tonhäuser, K. Woldmann, S. Ripperger, J. W. Tichy, *Chem. Ing. Tech.* **2004**, *76 (12)*, 114–118. DOI: https://doi.org/10.1002/cite.200403279

[37] J. W. Daily, R. E. Nece, *J. Basic Eng.* **1960**, *82 (1)*, 217–230. DOI: https://doi.org/10.1115/1.3662532

[38] P. Cooper, E. Reshotko, *AIAA J.* **1975**, *13 (5)*, 573–578.

[39] H. N. Ketola, J. M. McGrew, *J. Lubr. Technol.* **1968**, *90 (2)*, 395–404. DOI: https://doi.org/10.1115/1.3601573

[40] B. Schiele, *Dissertation*, Universität Stuttgart (TH) **1979**.

[41] W. H. Herschel, R. Bulkley, *Kolloid-Z.* **1926**, *39 (4)*, 291–300. DOI: https://doi.org/10.1007/BF01432034

[42] D. Goldnik, R. Weiler, S. Ripperger, G. Grim, *Filtr. Sep. Int. Ed.* **2012**, *12*, 19–23.

[43] L. Steinke, S. Ripperger, *Chem. Eng. Technol.* **2010**, *33 (8)*, 1369–1376. DOI: https://doi.org/10.1002/ceat.201000150

